

Parity-Violating Pion-Nucleon Coupling $h_{\pi NN}^{(1)}$ from π^+ -Electroproton Production Near the Threshold

Jiunn-Wei Chen and Xiangdong Ji

Department of Physics, University of Maryland, College Park, MD 20742-4111

Abstract

We study the possibility of measuring parity-violating pion-nucleon coupling $h_{\pi NN}^{(1)}$ from π^+ -electroproton production in the threshold region. We calculate the electron-helicity asymmetry in terms of $h_{\pi NN}^{(1)}$ and the Z-boson exchange between the electron and proton in leading-order heavy-baryon chiral perturbation theory. From the result, we demonstrate that the coupling can be determined to an accuracy of $\sim 2 \times 10^{-7}$ in an experiment with incident electron energy 250 MeV, luminosity 10^{38} $\text{sec}^{-1} \text{cm}^{-2}$, and a running time of 10^7 sec.

Weak interaction effects in hadron structure and reactions are usually masked by much stronger strong and electromagnetic interactions. Only under special circumstances can they be studied through high-precision measurements of observables vanishing in the absence of weak processes. The cross section asymmetry originating from a single longitudinal polarization is such an observable. At low energy, parity-violating hadronic interactions can be systematically classified in the framework of effective field theories [1–3]. In chiral power counting, the most important is the isovector P-odd pion-nucleon coupling $h_{\pi NN}^{(1)}$ which is responsible for the longest range part of the parity-violating $\Delta I = 1$ NN forces [1,4,5], the nucleon and nuclear anapole moments [6–11]. In quantum chromodynamics (QCD), its value is believed to be dominated by the s -quark contribution generated from the neutral current interaction [12]. Clearly, $h_{\pi NN}^{(1)}$ is one of the most important observables that characterize the size of the nonleptonic weak interactions in hadron systems.

In the last two decades, serious attempts have been made to pin down $h_{\pi NN}^{(1)}$, and as of to date, considerable uncertainty remains. Reviews of the experimental and theoretical status at the different stages of investigation can be found in [5,13,14]. In many-body systems, parity-violating effects can be enhanced significantly by important many-body correlations and have been detected experimentally. However, because of the underlying theoretical uncertainty, they cannot be translated easily into the corresponding results for the fundamental parameters. A large discrepancy exists on the extracted parity-violating coupling from the gamma asymmetry A_γ from the polarized ^{18}F decay [15] and from the anapole moment measurement in ^{133}Cs atom [16]. In few-body systems, the theory is under better control; but the parity-violating effects are generally small. The existing experimental results, and hence the extracted parameters, have very large error bars [17]. New

high-precision experiments currently under way are expected to overcome the problem of accuracy. These include $\vec{n}p \rightarrow d\gamma$ at LANSCE [18], $\vec{\gamma}d \rightarrow np$ at Jefferson Lab (JLab) [19] (however, see Ref. [20] for a different opinion on the sensitivity of this channel to $h_{\pi NN}^{(1)}$), and the rotation of polarized neutrons in helium at NIST [17]. Parity-violating observables related to a single nucleon are free of nucleon-nucleon interactions and thus have important advantages. In addition, heavy-baryon chiral perturbation theory (HB χ PT) provides a rigorous tool for making theoretical analyses. Recently, Bedaque and Savage, and Chen, Cohen and Kao have studied parity-violating effects in Compton scattering with a polarized target [21] or a polarized beam [22]. In Ref. [23], the present authors have studied extraction of $h_{\pi NN}^{(1)}$ in the pion photoproton production, $\vec{\gamma}p \rightarrow n\pi^+$ at the threshold region. While all these processes are easy to analyze theoretically, the experimental practicality requires them to have a large unpolarized cross section and large parity-violating asymmetries. In these regards, the pion production is more attractive.

Following our previous work mentioned above [23], we consider in this paper the measurement of $h_{\pi NN}^{(1)}$ from π^+ production in low-energy electron-proton scattering. Since the momenta involved in the process are constrained to be much smaller than the nucleon mass, a leading-order (LO) calculation in HB χ PT is appropriate within 30% uncertainty [2,3]. Theoretical studies of the same process have been carried out previously by Li, Henley and Hwang and by Hammer and Drechsel by considering the predominant Z boson exchange effects in the context of meson exchange models [24,25]. The goal of the present study is to use $ep \rightarrow e'\pi^+n$ to measure the leading hadronic parity-violating coupling, and therefore we focus mainly on the threshold region where the effect of $h_{\pi NN}$ is important and where HB χ PT applies.

The process that we are interested in is

$$\vec{e}(k) + p(P_i) \rightarrow e(k') + \pi^+(k_\pi) + n(P_f) , \quad (1)$$

where $k^\mu = (E_e, \vec{k})$, P_i^μ , $k'^\mu = (E'_e, \vec{k}')$, $k_\pi^\mu = (\omega_\pi, \vec{k}_\pi)$, and P_f^μ are the laboratory four-momenta of the initial electron, proton, final electron, pion, and neutron, respectively. The interaction between the electron and the hadrons is treated in the Bonn approximation, and the four-momentum of the intermediate vector boson γ or Z is denoted as $q = k - k'$. To justify the use of chiral perturbation theory, we require the four-momenta of the virtual vector boson and pion and three-momentum of the nucleon be small as compared to the nucleon mass scale M_N .

We first consider the unpolarized pion production cross section without weak interactions. In Fig. 1, we have shown the complete leading-order (LO) (group (a)) and part of the next-to-leading order (NLO) (group (b)) Feynman diagrams in HB χ PT, where electron lines have been omitted, the wavy lines represent the virtual photons, solid lines the nucleons, dashed lines the pions, and the double lines the Δ resonances. The solid circles denote the NLO vertices. The differential cross section after integrating over the final neutron momentum can be written as

$$\frac{d\sigma}{dE'd\Omega'} = \frac{2\alpha_{\text{em}}^2 E' M_N}{Q^4 E} \mathcal{M} \delta((P_i + q - k_\pi)^2 - M_N^2) \frac{d^3 \vec{k}_\pi}{(2\pi)^3 2\omega_\pi} , \quad (2)$$

where $Q^2 = -q^2$ and

$$\begin{aligned} \mathcal{M} &= \ell^{\mu\nu} W_{\mu\nu} , \\ W_{\mu\nu} &= \langle p(P_i) | J_\mu | n(P_f) \pi(k_\pi) \rangle \langle n(P_f) \pi(k_\pi) | J_\nu | p(P_i) \rangle , \end{aligned} \quad (3)$$

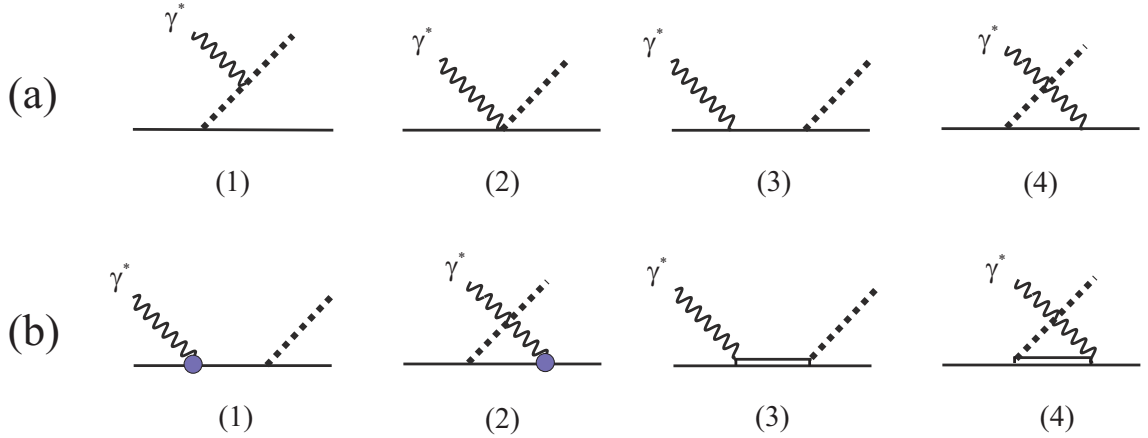


FIG. 1. Leading order (a) and next-to-leading order (b) Feynman diagrams for unpolarized π^+ electroproduction from a proton. The electron lines have been omitted and the delta resonance is represented by double lines. The solid circles denote the next-to-leading order vertices. The group (b) is incomplete but sufficient for the purpose of this paper.

with $P_f = P_i + q - k_\pi$. The unpolarized lepton tensor is $\ell^{\mu\nu} = (1/2)\text{Tr}[k\gamma^\mu k'\gamma^\nu] = 2(k^\mu k'^\nu + k^\nu k'^\mu - g^{\mu\nu}k' \cdot k)$. The hadron tensor $W^{\mu\nu}$ depends on the matrix elements of the electromagnetic current between the hadron states. From the LO diagrams, we find

$$\begin{aligned}
W^{\mu\nu} = & \frac{g_A^2}{2f_\pi^2} \left[(2k_\pi - q)^\mu (2k_\pi - q)^\nu \frac{|\vec{k}_\pi - \vec{q}|^2}{((k_\pi - q)^2 - m_\pi^2)^2} \right. \\
& + \frac{\vec{k}_\pi \cdot (\vec{k}_\pi - \vec{q})}{\omega((k_\pi - q)^2 - m_\pi^2)} [v^\mu (2k_\pi - q)^\nu + v^\nu (2k_\pi - q)^\mu] \\
& - \frac{1}{(k_\pi - q)^2 - m_\pi^2} [((2k_\pi - q)^\mu v^\nu + (2k_\pi - q)^\nu v^\mu) v \cdot (k_\pi - q) \\
& - (2k_\pi - q)^\mu (k_\pi - q)^\nu - (2k_\pi - q)^\nu (k_\pi - q)^\mu] \\
& \left. \left(1 + \frac{|\vec{k}_\pi|^2}{\omega^2} - \frac{2\omega_\pi}{\omega} \right) v^\mu v^\nu - g^{\mu\nu} + \frac{1}{\omega} (v^\mu k_\pi^\nu - v^\nu k_\pi^\mu) \right], \quad (4)
\end{aligned}$$

where $v^\mu = (1, 0, 0, 0)$ is the velocity of the nucleon at rest, $g_A = 1.257$ is the neutron-decay constant, and $f_\pi = 93$ MeV is the pion decay constant. As expected $W^{\mu\nu}$ is symmetric in μ and ν , and satisfies the current conservation: $W^{\mu\nu}q_\mu = 0$.

For the process to be useful in probing small parity-violating effects, the cross section must be sizable enough to yield a large number of events ($\sim 10^{14}$) in a realistic experiment. For an estimate, it is sufficient to examine the LO theoretical prediction. In Fig. 2(a), we have shown the cross section as a function of the scattered electron energy after all other variables are integrated. The solid curve is the result with the incident electron energy $E_e = 200$ MeV, and the dashed one with $E_e = 250$ MeV. In the former case, the scattered electron energy is peaked around 20 MeV, and in the latter, it ranges from 20 to 80 MeV. In principle, the electrons from elastic scattering off the protons have much higher energy. When taking into account quantum electrodynamics

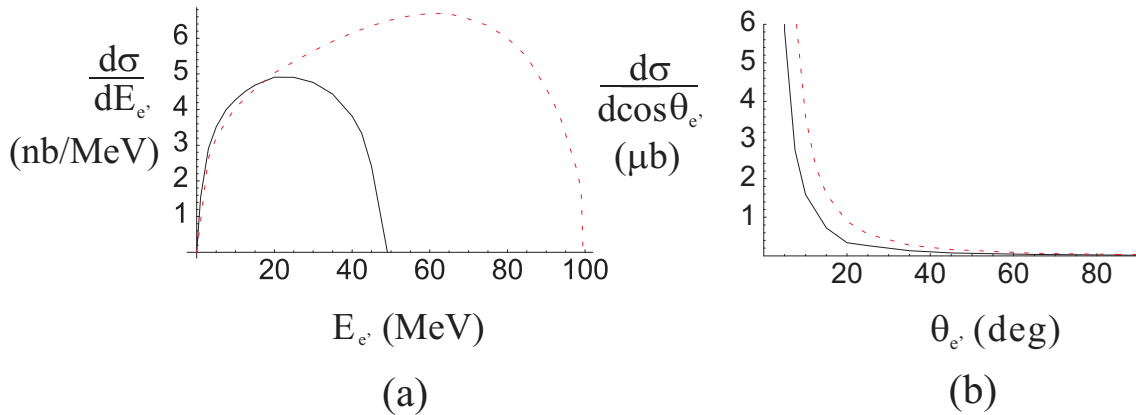


FIG. 2. Pion-production cross section as a function of the scattered electron energy (a) and polar angle (b) at the incident electron energy $E_e = 200$ (solid line) and 250 MeV (dashed line), respectively.

bremsstrahlung, however, the elastic peak has a well-known tail which contaminates the electron spectrum from pion production. In Fig. 2(b), we have shown the cross section as a function of the scattered electron angle. As expected, the cross section is forward peaked due to the infrared factor $1/Q^4$ in Eq. (2). For both beam energies, most electrons are scattered into a polar angle less than 10° .

Because of the large number of events needed in parity-violating experiments, coincidence detection is not an option. For $ep \rightarrow e'\pi^+n$, the best possibility may be π^+ semi-inclusive detection. In Fig. 3(a), we have shown the integrated cross section as a function of the energy of the pion yield. At $E_e = 200$ MeV, the pion energy is peaked around $\omega_\pi = 155$ MeV, which translates to a pion momentum ~ 65 MeV, or $\beta = v/c \sim 0.45$. Therefore, the pion decay length is about 3.5 m, and most pions can be detected before their weak decays. At $E_e = 250$ MeV, the pion energy is peaked around 170 MeV. In Fig. 3(b), we have shown the pion angular distribution in lab frame. At backward angles, the production rate is about a factor of 3 smaller than that at the forward angles. This reduction is mainly due to the Lorentz boost. According to the figure, the semi-inclusive pion production cross section is about 100nb at a forward steradian and at $E_e = 250$ MeV. To produce 10^7 events per second needed in a useful and practical experiment, the luminosity must be at least $10^{38} \text{ sec}^{-1} \cdot \text{cm}^{-2}$. Although the lower limit is not difficult to achieve, a high-statistics measurement may require much higher luminosity, making the experiment challenging.

Given the sizable rate for π^+ production in e - p scattering, we now analyze the parity-violating effects. According to the standard electroweak theory, parity violation in $\vec{e}p \rightarrow e'\pi^+n$ comes from two distinct sources. First, the non-leptonic weak interactions generate parity violation hadronic vertices. At low energy, these vertices can be classified systematically in terms of chiral power counting [1]. To $\mathcal{O}(p^0)$ (ignore the weak coupling in power counting), it has one term,

$$\mathcal{L}^{PV} = -ih_{\pi NN}^{(1)}\pi^+p^\dagger n + h.c. + \dots, \quad (5)$$

where the ellipses denote terms with more pion fields and derivatives, and the phase convention is taken from Refs. [10,11]. The complete leading (group (a)) and part of the next-to-leading (group (b)) order Feynman diagrams involving $h_{\pi NN}^{(1)}$ are shown in Fig. 4. The contribution involving

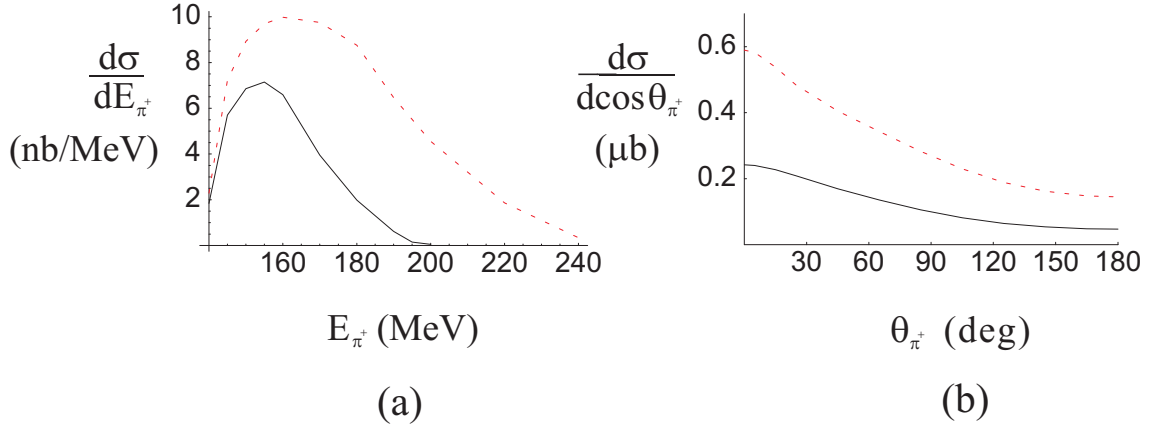


FIG. 3. Pion-production cross section as a function of the outgoing pion energy (a) and polar angle (b) at the incident electron energy $E_e = 200$ (solid line) and 250 MeV (dashed line), respectively.

the intermediate delta resonance comes in at higher orders. The second source of parity-violation is the semi-leptonic process of Z-boson exchange between the scattering electron and the nucleon system. The relevant Feynman diagrams are shown in group (c) of Fig. 4. Since $\sin^2\theta_W \sim 1/4$, we approximate the Z-electron coupling as pure axial, and the Z-quark coupling pure vector.

The leading hadronic parity-violating contribution comes from the interference of the LO parity-conserving and LO parity-violating amplitudes; the result depends on the nucleon polarization. For polarized electron scattering on unpolarized proton, the lepton tensor is $l_{\mu\nu} = 2i\epsilon^{\mu\nu\alpha\beta}k_\alpha k'_\beta$ for helicity + electron; the leading P-odd contribution comes from the interference between the LO (NLO) parity-conserving and NLO (LO) parity-violating amplitudes. Although the NLO diagrams in Figs. 1(b) and 4(b) are incomplete, they are sufficient for calculating this P-odd contribution. The resulting hadron tensor $W^{\mu\nu}$ is

$$\begin{aligned}
W^{\mu\nu} = & -\frac{ig_A h_{\pi NN}^{(1)}}{\sqrt{2}f_\pi M_N \omega} \left\{ \epsilon^{\mu\nu\alpha\beta} q_\alpha v_\beta \left(\mu_p - \frac{\omega}{\omega_\pi} \mu_n \right) \right. \\
& + \left[\epsilon^{\mu\nu\alpha\beta} q_\alpha v_\beta \left(\frac{2m_\pi^2 - q \cdot k_\pi}{(k_\pi - q)^2 - m_\pi^2} + \frac{\omega_\pi}{\omega} \right) \right. \\
& \left. \left. + \epsilon^{\mu\nu\alpha\beta} k_{\pi\alpha} q_\beta \left(\frac{2\omega_\pi - \omega}{(k_\pi - q)^2 - m_\pi^2} + \frac{1}{\omega} \right) \right] \right. \\
& \left. \times \left[-\left(\mu_p - \frac{\omega}{\omega_\pi} \mu_n \right) + \frac{2g_{\pi N\Delta} G_1}{9g_A} \left(\frac{\omega}{\omega - \Delta} + \frac{\omega}{\omega_\pi + \Delta} \right) \right] \right\}, \quad (6)
\end{aligned}$$

which is conserved and antisymmetric in μ and ν . Parameter Δ is the mass difference between the nucleon and delta resonance, and is treated as small as compared to M_N . $\mu_{p,n}$ is the magnetic moment of the proton and neutron in units of the nuclear magnetons, respectively. $G_1 = 3.85$ and $g_{\pi N\Delta} = 1.05$ are the γ - N - Δ and the π - N - Δ coupling constants [26].

As mentioned above, the semi-leptonic parity-violating contribution comes from the Z-exchange between the scattering electron and the nucleon system. Taking into account only the axial coupling from the electron, the parity-violating S-matrix element is

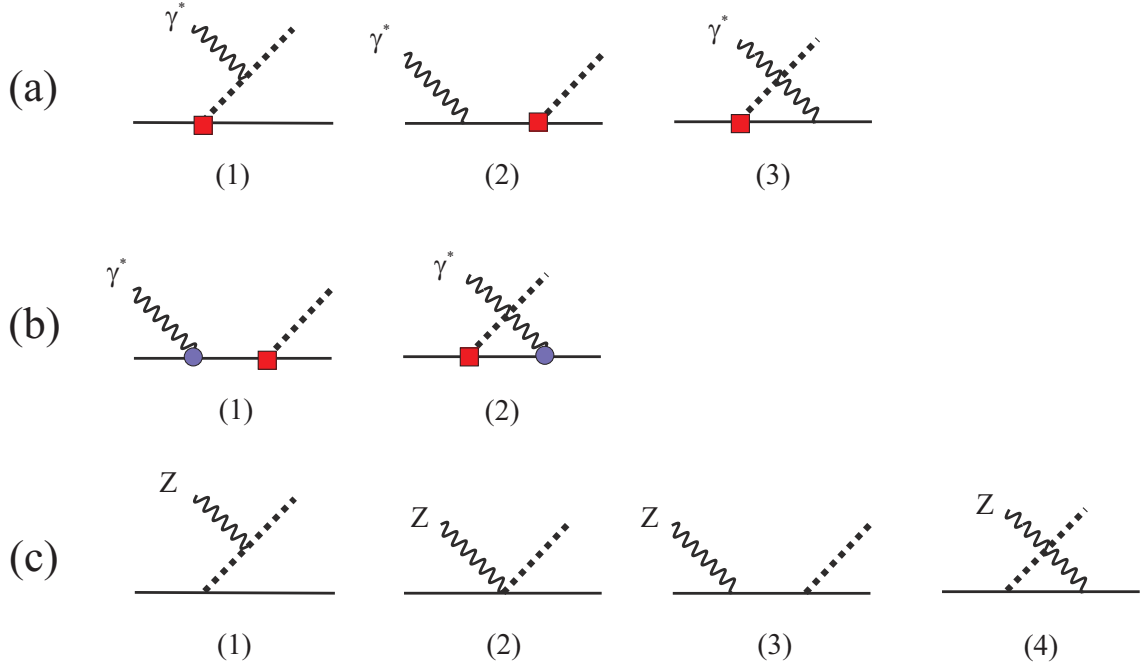


FIG. 4. Feynman diagrams contributing to the parity-violating amplitudes at LO and NLO in $\vec{e}'p \rightarrow e'\pi^+n$.

$$\langle e'\pi^+n|S|ep\rangle = -i(2\pi)^4\delta^4(k + P_i - k' - k_\pi - P_f)\frac{G_F}{\sqrt{2}}\bar{e}(k')\gamma^\mu\gamma_5 e(k)\langle\pi^+n|J_\mu^Z|p\rangle, \quad (7)$$

where $J^{Z\mu}$ is the vector part of the quark neutral current: $\bar{u}\gamma^\mu u(1/2 - 4/3\sin^2\theta_W) + \bar{d}\gamma^\mu d(-1/2 + 2/3\sin^2\theta_W) + \dots$. The LO matrix element $\langle\pi^+n|J_\mu^Z|p\rangle$ in HB χ PT can be calculated from Feynman diagrams shown in Fig. 4(c). After approximating $\omega = \omega_\pi$, the resulting parity-violating cross section is directly proportional to the LO spin-independent cross section,

$$d\sigma^{\text{PV from Z}} = -2\sqrt{2}(1 - 2\sin^2\theta_W)\frac{G_F Q^2}{4\pi\alpha_{\text{em}}}d\sigma^{\text{PC at LO}}. \quad (8)$$

One can calculate the Z-exchange more accurately by including the electron vector-current contribution and going to NLO in HB χ PT. For our purpose, however, the above accuracy is sufficient.

In Fig. 5(a), we have shown the electron-helicity asymmetry (defined as the difference between the positive and negative helicity cross sections normalized to the sum) as a function of the polar angle of the pion in the laboratory frame. For $E_e = 200$ MeV, the asymmetry from Z-exchange (dashed line) is on the order of -2.5×10^{-7} with small angular dependence. Assuming the “best guess” for $h_{\pi NN}^{(1)} = 5 \times 10^{-7}$ [4], the hadronic parity-violating contribution cancels this almost entirely, as shown by the solid curve. The cancelation shows that, at this low energy, the two contributions have the same order of magnitude. As a result, the total parity-violating asymmetry is difficult to measure. When the scattering electron energy is increased to 250 MeV, the asymmetry from Z-exchange is increased by approximately a factor of 2 because of the larger Q^2 , whereas the contribution from $h_{\pi NN}^{(1)}$ changes little, as shown in Fig. 5(b). The combined asymmetry is now negative, and has a sizable magnitude around -2×10^{-7} .

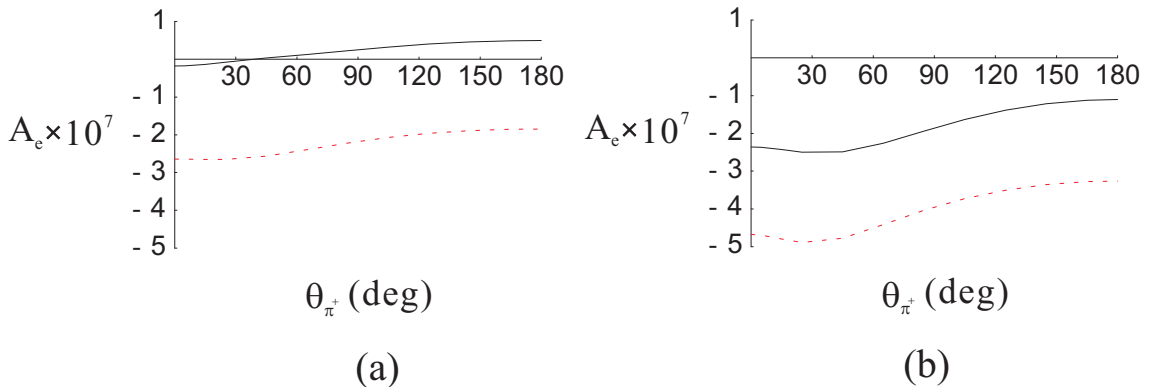


FIG. 5. The electron helicity asymmetry A_e as a function of outgoing-pion polar angle at $E_e = 200$ (a) and 250 MeV (b). The dashed lines include the Z contributions only, whereas the solid lines include the contribution from $h_{\pi NN}^{(1)}$ (taken to be 5×10^{-7}) as well.

We have also shown the asymmetry as a function of the pion energy in Fig. 6. When the incident electron energy is 200 MeV, the total asymmetry is again small. This is particularly true for most of the pions that are produced with 160 MeV energy. When the electron energy is 250 MeV, the cancellation between the Z-exchange and hadronic parity-violation is not complete. For a large fraction of pions which are produced with energy between 160 and 180 MeV, the asymmetry is significant. Therefore, the best way to extract $h_{\pi NN}^{(1)}$ from $ep \rightarrow e\pi^+n$ is to measure pion production asymmetry in the forward direction with a polarized electron beam of 250 MeV.

For the incident electron energy of 250 MeV, the virtual photon energy is around 200 MeV (see fig. 2(a)). According to our previous study [23], the unpolarized cross section at this energy can be described well by the LO HB χ PT calculation. Therefore, the applicability of chiral perturbation theory in studying the parity violating effects in the electroproduction is qualitatively similar to that in photoproduction. In particular, we believe that the higher-order corrections are $\mathcal{O}(\epsilon/m_N)$, where ϵ stands for m_π , ω , ω_π , and Δ .

To summarize, we have studied the possibility of measuring the parity-violating coupling $h_{\pi NN}^{(1)}$ from semi-inclusive π^+ electroproduction on the proton target in the threshold region. For the incident energy of 250 MeV, the electron single-spin asymmetry is estimated around -2×10^{-7} in the forward direction. This asymmetry can be measured to an accuracy of 50% (this implies an accuracy of 2×10^{-7} in $h_{\pi NN}^{(1)}$) with a luminosity of $10^{38} \text{ sec}^{-1} \cdot \text{cm}^{-2}$ and a running time of 10^7 sec. A more careful study of the higher-order effects will be published later [27].

ACKNOWLEDGMENTS

We thank D. Beck, E. Beise, E.M. Henley, R. McKeown, R. Suleiman, and B. Wojtsekhowski for discussions on the experimental issues. We also thank C. Jung for help with the numerical calculations. This work is supported in part by the U.S. Dept. of Energy under grant No. DE-FG02-93ER-40762.

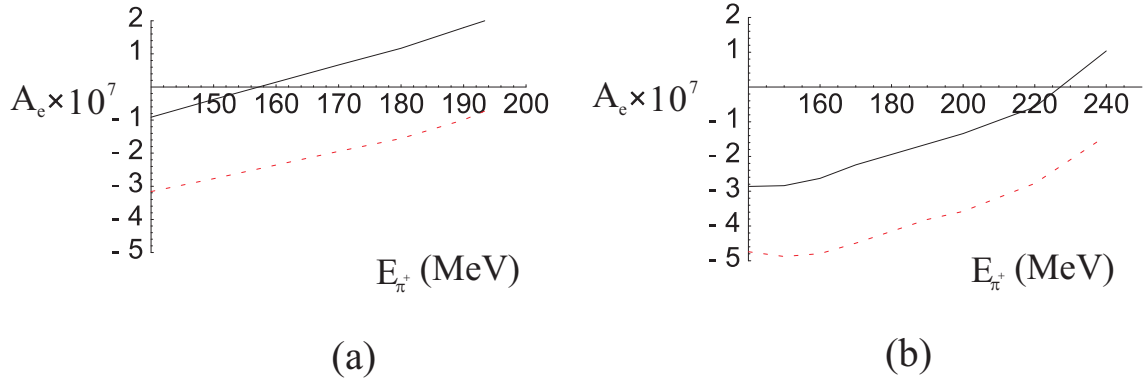


FIG. 6. The electron-helicity asymmetry A_e as a function of the pion energy at (a) $E_e = 200$ and (b) 250 MeV. The curves have the same significance as in Fig. 5.

REFERENCES

- [1] D.B. Kaplan and M.J. Savage, *Nucl. Phys. A* **556**, 653 (1993).
- [2] E. Jenkins and A. V. Manohar, *Phys. Lett. B* **255**, 558 (1991).
- [3] V. Bernard, N. Kaiser and Ulf-G. Meissner, *Int. J. Mod. Phys. E* **4**, 193 (1995).
- [4] B. Desplanques, J.F. Donoghue and B.R. Holstein, *Ann. Phys. (N.Y.)* **124**, 449 (1980).
- [5] E.G. Adelberger and W.C. Haxton, *Ann. Rev. Nucl. Part. Sci.* **35**, 501 (1985).
- [6] Y.B. Zel'dovich, *Sov. Phys. JETP* **6**, 1184 (1958); *Sov. Phys. JETP* **12**, 777 (1961).
- [7] W.C. Haxton, E.M. Henley and M.J. Musolf, *Phys. Rev. Lett.* **63**, 949 (1989).
- [8] M.J. Musolf and B.R. Holstein, *Phys. Rev. D* **43**, 2956 (1991).
- [9] M.J. Savage and R.P. Springer *Nucl. Phys. A* **644**, 635 (1998), *Erratum-ibid. A* **657**, 457 (1999); [nucl-th/9907069](#).
- [10] C.M. Maekawa and U. van Kolck, *Phys. Lett. B* **478**, 73 (2000); C.M. Maekawa, J.S. Veiga and U. van Kolck, *Phys. Lett. B* **488**, 167 (2000).
- [11] S.-L. Zhu, S.J. Puglia, B.R. Holstein and M.J. Ramsey-Musolf, *Phys. Rev. D* **62**, 033008 (2000); [hep-ph/0005281](#)
- [12] J. Dai, M.J. Savage, J. Liu and R. Springer, *Phys. Lett. B* **271**, 403 (1991).
- [13] W. Haeberli, B.R. Holstein, in *Symmetries and Fundamental Interactions in Nuclei*, ed. W.C. Haxton and E.M. Henley (World Scientific, Singapore, 1995), p.17.
- [14] W.T.H. van Oers, *Int. J. Mod. Phys. E* **8**, 417 (1999).
- [15] S.A. Page *et al.*, *Phys. Rev. C* **35**, 1119 (1987); M. Bini, T. F. Fazzini, G. Poggi, and N. Taccetti, *Phys. Rev. C* **38**, 1195 (1988).
- [16] C.S. Wood *et al.*, *Science* **275**, 1759 (1997); W.C. Haxton, *Science* **275**, 1753 (1997); V.V. Flambaum and D.W. Murray, *Phys. Rev. C* **56**, 1641 (1997); W.S. Wilburn and J.D. Bowman, *Phys. Rev. C* **57**, 3425 (1998).
- [17] V.A. Knyazkov *et al.*, *Nucl. Phys. A* **417**, 209 (1984); J.F. Cavagnac, B. Vignon and R. Wilson, *Phys. Lett. B* **67**, 148 (1997); D.M. Markoff, Ph.D. Thesis, University of Washington (1997).
- [18] W.M. Snow *et al.*, *Nucl. Inst. Meth. A* **440**, 729 (2000).
- [19] JLab LOI 00-002, W. van Oers and B. Wojtsekhowski, spokesmen.
- [20] I.B. Khriplovich and R.V. Korkin, [nucl-th/0010032](#).

- [21] P.F. Bedaque and M.J. Savage, *Phys. Rev. C* **62**, 018501 (2000).
- [22] J.W. Chen, T.D. Cohen and C.W. Kao, nucl-th/0009031.
- [23] J.W. Chen and X. Ji, hep-ph/0011230.
- [24] S.P. Li, E.M. Henley and W-Y. P. Hwang, *Ann. Phys.* **143**, 372 (1982).
- [25] H.W. Hammer and D. Drechsel, *Z. Phys. A* **353**, 321 (1995).
- [26] T.R. Hemmert, University of Massachusetts Ph.D. Thesis, Amherst 1997; T.R. Hemmert, B.R. Holstein, G. Knochlein and D. Drechsel, *Phys. Rev. D* **62**, 014013 (2000).
- [27] J.W. Chen and X. Ji, to be published.